



STRUCTURAL DAMAGE DETECTION BY A SENSITIVITY AND STATISTICAL-BASED METHOD

A. MESSINA

Dipartimento di Scienza dei Materiali, Università di Lecce, Lecce, Italy

E. J. WILLIAMS

*Department of Mechanical Engineering, University of Nottingham,
Nottingham NG7 2RD, U.K.*

AND

T. CONTURSI

*Dipartimento di Progettazione e Produzione Industriale, Politecnico di Bari, Bari,
Italy*

(Received 15 July 1996, and in final form 8 April 1998)

During the last 20 years, the development of experimental modal analysis techniques has facilitated the accurate measurement of modal parameters in many types of structure. Alongside this work, several methods have been developed to detect structural damage by using location-dependent changes in the modal parameters. The paper extends the authors' work on a correlation coefficient termed the Multiple Damage Location Assurance Criterion (MDLAC) by introducing two methods of estimating the size of defects in a structure. Their effectiveness is illustrated using numerical data for two truss structures and both location and sizing algorithms are validated experimentally using a three-beam test structure. The paper also introduces a means of improving the computational efficiency of the damage location algorithm. The MDLAC approach offers the practical attraction of only requiring measurements of the changes in a few of the structure's natural frequencies between the undamaged and damaged states and is shown to provide good predictions of both the location and absolute size of damage at one or more sites.

© 1998 Academic Press

1. INTRODUCTION

Recently, much work has been dedicated to solving the problem of detecting the location and extent of damage in elastic structures by using the changes in their modal parameters; specifically, the natural frequencies, modal damping and associated mode shapes. It is widely recognized that the natural frequencies are

least contaminated by measurement noise and can generally be measured with good accuracy. Messina *et al.* [1] suggest a standard error of $\pm 0.15\%$ as a benchmark figure for natural frequencies measured in the laboratory with the impulse hammer technique. In contrast, modal damping and mode shape estimates have error levels as much as 20 times worse [2] than those in the corresponding natural frequency estimates.

In practice, measurements yield only partial mode shapes with respect to the total degrees of freedom (DOFs) present in corresponding finite element (FE) models. While the use of expansion methods [3, 4] can assist, the ratio of measured to analytical DOFs is invariably low with consequential errors in the assessment of the mode shapes. These difficulties are compounded when the structure under test exhibits complex mode shapes and the FE model being used for the expansion produces normal modes.

A number of non-destructive evaluation techniques based on changes in a structure's modal parameters have been introduced. Cawley and Adams [5] used the changes in the natural frequencies together with a FE model to locate the damage site. Some researchers [1, 6] have found this method susceptible to measurement errors and ways of improving the localization have been proposed [7]. Experiments performed by Biswas *et al.* [8] on a highway bridge also demonstrated that changes in the natural frequencies alone could be used to detect damage. Other authors [9, 10] have described similar success.

By including mode shape information, several authors have developed methods of assessing the extent of damage in addition to its location. Pandey and Biswas [11] used complete mode shapes for the damaged and undamaged states to identify both the location and amount of damage in a single pass by solving a system of linear equations. Zimmerman and Kaouk's algorithm [12] used two passes, the first to locate the damage site and the second to assess the amount of damage. Topole and Stubbs [13] also used mode shapes and natural frequencies and showed the importance of introducing mode shape orthogonality to identify the location and extent of damage on a structure by a pseudo-inverse solution of a system of linear equations.

In practice, only a truncated set of natural frequencies and partial mode shapes can be expected experimentally. As a result, a method capable of predicting the extent as well as the location of damage that requires only the changes in the natural frequencies would be welcomed.

Messina *et al.* proposed an assurance criterion for detecting single damage sites [1] and this was extended [14, 15] to identify the relative amount of damage at multiple sites. The principles were demonstrated on numerical test cases using error-free data. This paper extends the approach further to give an absolute assessment of the amount of damage present and validates the practical application of the method with an experimental investigation. It will be seen in section 2.2 that the solution procedure can involve significant computational effort when analyzing large structures and section 3.3 therefore introduces a method of dramatically reducing the solution time. Before describing the new work, the basis for the MDLAC approach will be briefly reviewed.

2. DAMAGE DETECTION PRINCIPLE

2.1. LOCATION OF DAMAGE AT A SINGLE SITE

If $\{\Delta \mathbf{f}\}$ is the measured frequency change vector for a structure with a single defect of unknown size or location and $\{\delta \mathbf{f}_j\}$ is the theoretical frequency change vector for damage of a known size at location j , the Damage Location Assurance Criterion (DLAC) for location j can be defined using a correlation approach similar to the modal assurance criterion (MAC) used for comparing mode shape vectors.

$$\text{DLAC}(j) = \frac{|\{\Delta \mathbf{f}\}^T \cdot \{\delta \mathbf{f}_j\}|^2}{(\{\Delta \mathbf{f}\}^T \cdot \{\Delta \mathbf{f}\}) \cdot (\{\delta \mathbf{f}_j\}^T \cdot \{\delta \mathbf{f}_j\})}. \quad (1)$$

As can be seen from the Cauchy–Schwarz inequality, DLAC values lie in the range of 0 to 1, with 0 indicating no correlation and 1 indicating an exact match between the patterns of frequency changes. The location j giving the highest DLAC value gives the best match to the measured frequency change pattern and is therefore taken as the predicted damage site. It is found [1] that a more accurate localization can be obtained if the frequency changes are normalized with respect to the frequency of the undamaged structure. This is because the use of percentage changes gives similar weight to all modes, whereas the use of absolute frequency changes favours the higher modes since these tend to exhibit larger shifts. Percentage changes are used throughout the work reported here.

As with the MAC parameter, equation (1) provides a sound statistical measure to discriminate between the patterns for each potential damage site. Tests [1] have shown that only about 10 to 15 modes are required to give sufficient discrimination for reliable damage localization. This is an important advantage of the method since higher-frequency mode shapes can change significantly when damage occurs and can make it difficult in practice to match the modal pairs from undamaged to damaged states. The modest mode number requirement makes mode-matching errors less likely.

The original DLAC code was shown [1] to be robust in the presence of measurement error and to give the correct location for damage of a range of sizes at a single site.

2.2. LOCATION OF DAMAGE AT MULTIPLE SITES

The DLAC formulation applies to single defects only, but can be extended to multiple sites by making use of an analytical model of the structure.

The model is based on the sensitivity of the frequency of each mode to damage in each location. To calculate the sensitivities, it is assumed that damage to the j th element is simulated by a homogeneous reduction of stiffness, but with no change of mass. In this case, the sensitivity of the k th natural frequency to damage at location j is given by equation (2) below.

$$\frac{\partial f_k}{\partial D_j} = \frac{1}{8 \cdot f_k^0 \cdot \pi^2} \cdot \frac{\{\Phi_k^0\}^T [\mathbf{K}_j^0] \{\Phi_k^0\}}{\{\Phi_k^0\}^T [\mathbf{M}^0] \{\Phi_k^0\}}, \quad (2)$$

where $[\mathbf{K}_j^e]$ is the stiffness matrix of the j th element positioned within the global matrix, $[\mathbf{M}^o]$ is the global mass matrix and $\{\boldsymbol{\phi}_k^e\}$ is the k th mode shape vector; all terms evaluated are for the undamaged structure.

A stiffness reduction factor D_j for the element is introduced such that $D_j = 1$ for no damage and $D_j = 0$ for complete loss of the element (100% damage). For any combination of size and location of damage at one or more sites (embodied in a vector of changes to individual stiffness reduction factors $\{\delta\mathbf{D}\}$), it is assumed that the corresponding reductions in the natural frequencies can be written using a linear combination of the sensitivities in the form:

$$\begin{aligned}\delta f_1 &= \frac{\partial f_1}{\partial D_1} \delta D_1 + \frac{\partial f_1}{\partial D_2} \delta D_2 + \cdots + \frac{\partial f_1}{\partial D_m} \delta D_m \\ &\quad \dots\dots\dots \\\delta f_p &= \frac{\partial f_p}{\partial D_1} \delta D_1 + \frac{\partial f_p}{\partial D_2} \delta D_2 + \cdots + \frac{\partial f_p}{\partial D_m} \delta D_m\end{aligned}$$

$$\text{or } \{\delta\mathbf{f}\} = \begin{bmatrix} \frac{\partial f_1}{\partial D_1} & \cdots & \frac{\partial f_1}{\partial D_m} \\ \cdots & \cdots & \cdots \\ \frac{\partial f_p}{\partial D_1} & \cdots & \frac{\partial f_p}{\partial D_m} \end{bmatrix} \{\delta\mathbf{D}\}, \quad (3)$$

or

$$\{\delta\mathbf{f}\} = [\mathbf{S}]\{\delta\mathbf{D}\}.$$

Equation (3) gives the analytical predictions of the frequency changes, $\{\delta\mathbf{f}\}$, resulting from an arbitrary pattern of damage defined by the vector $\{\delta\mathbf{D}\}$. Substituting this into equation (1), one obtains a statistical correlation with the measured frequency changes, $\{\Delta\mathbf{f}\}$. This is termed the Multiple Damage Location Assurance Criterion (MDLAC) since it is a function of all elements in the damage vector $\{\delta\mathbf{D}\}$.

$$\text{MDLAC}(\{\delta\mathbf{D}\}) = \frac{|\{\Delta\mathbf{f}\}^T \cdot \{\delta\mathbf{f}(\{\delta\mathbf{D}\})\}|^2}{(\{\Delta\mathbf{f}\}^T \cdot \{\Delta\mathbf{f}\}) \cdot (\{\delta\mathbf{f}(\{\delta\mathbf{D}\})\}^T \cdot \{\delta\mathbf{f}(\{\delta\mathbf{D}\})\})}. \quad (4)$$

Using the same damage detection principle as before, the required damage state is obtained by searching for the vector $\{\delta\mathbf{D}\}$ which maximises the MDLAC value. The search is initiated by setting the damage vector $\{\delta\mathbf{D}\}$ to $\{0.01\% \}$. This is chosen to be close to, but not at, the undamaged state since $\{\delta\mathbf{D}\} = \{\mathbf{0}\}$ is a singular point for equation (4).

It will be noted that the size of $\{\delta\mathbf{f}\}$ is equal to the number of modes used, while the size of $\{\delta\mathbf{D}\}$ is equal to the number of potential damaged sites. The latter is a key factor in determining the computational time required for the search for the maximum. In principle, all elements in the structure could be considered as

potential damaged sites. However, section 3.3 discusses a method of reducing computational effort by excluding locations that are unlikely to be damaged.

2.3. DAMAGE EXTENT

The MDLAC formulation provides a solution vector $\{\delta \mathbf{D}\}$ giving the relative amount of damage at each site, but not an absolute estimate. This is because the linear assumption embodied in equation (3) means that changing the solution vector by a constant will not change the MDLAC correlation value. However, since the actual frequency-change vector $\{\Delta \mathbf{f}\}$ is known, an absolute damage scaling coefficient, C , can be estimated such that $C \cdot \{\delta \mathbf{D}\}$ gives the actual percentage damage present. Two algorithms have been developed for this.

2.3.1. First order approximation

If the linear analytical model were an exact match to the experimental data, the predicted frequency changes given by equation (3) would be identical to the measured changes. That is:

$$\{\Delta \mathbf{f}\} = C \cdot [\mathbf{S}]\{\delta \mathbf{D}\}. \quad (5)$$

In principle, C could then be obtained from any one of the frequency-change values. For example, using mode k , one has;

$$C_k = \frac{\Delta f_k}{\{\mathbf{S}_k\} \cdot \{\delta \mathbf{D}\}}. \quad (6)$$

However, due to the first order assumption and the effects of errors in the measured frequencies, a more reliable value of the scaling coefficient is obtained by averaging the estimates from equation (6) for all of the modes used in the analysis.

2.3.2. Second order approximation

As damage increases, the effects of the true non-linear relation between frequency changes and damage can introduce significant errors in the size estimates. To combat this, a second order approximation has been developed.

For mode k , a second order approximation for the change in the eigenvalue λ_k can be obtained by expanding around the undamaged state using a Taylor series.

$$\lambda_k - \lambda_k^o = \left\{ \frac{\partial \lambda_k}{\partial D_1} \quad \dots \quad \frac{\partial \lambda_k}{\partial D_m} \right\} \times \begin{Bmatrix} \delta D_1 \\ \delta D_2 \\ \dots \\ \delta D_m \end{Bmatrix} + \frac{1}{2} \cdot \begin{Bmatrix} \delta D_1 \\ \delta D_2 \\ \dots \\ \delta D_m \end{Bmatrix}^T \cdot \begin{bmatrix} \frac{\partial^2 \lambda_k}{\partial D_1^2} & \dots & \frac{\partial^2 \lambda_k}{\partial D_1 \partial D_m} \\ \dots & \dots & \dots \\ \frac{\partial^2 \lambda_k}{\partial D_m \partial D_1} & \dots & \frac{\partial^2 \lambda_k}{\partial D_m^2} \end{bmatrix} \cdot \begin{Bmatrix} \delta D_1 \\ \delta D_2 \\ \dots \\ \delta D_m \end{Bmatrix} \quad (7)$$

or

$$\lambda_k = \lambda_k^o + \{\mathbf{s}_k\}\{\delta\mathbf{D}\} + \frac{1}{2}\{\delta\mathbf{D}\}^T[\mathbf{H}_k]\{\delta\mathbf{D}\} \quad \text{with } k = 1, \dots, p.$$

Lin and Lim [16] showed that the elements for the k th Hessian matrix, $[\mathbf{H}_k]$, used in equation (7) can be written as;

$$\left\{ \begin{array}{l} \frac{\partial^2 \lambda_k}{\partial D_j \partial D_i} = \sum_{\substack{r=1 \\ r \neq k}}^n (\lambda_k^o - \lambda_r^o) \cdot \beta(i)_{kr} \cdot [\beta(j)_{kr} - \beta(j)_{rk}] \\ \text{where } \beta(j)_{rk} = \frac{\{\Phi_r^o\}^T \cdot [\mathbf{K}_r] \cdot \{\Phi_k^o\}}{(\lambda_k^o - \lambda_r^o)}. \end{array} \right. \quad (8)$$

Equation (7) can then be used to obtain individual estimates of the scaling coefficient from each mode by solving quadratic equations in C_k in the form;

$$(\frac{1}{2}\{\delta\mathbf{D}\}^T[\mathbf{H}_k]\{\delta\mathbf{D}\})C_k^2 + (\{\mathbf{s}_k\}\{\delta\mathbf{D}\})C_k + (4\pi^2(f_k^{v^2} - f_k^2)) = 0. \quad (9)$$

Again, the final value for the absolute damage scaling coefficient is obtained by averaging the individual estimates.

3. ANALYTICAL EXAMPLES

3.1. ANALYTICAL MODELS

Two numerical examples are used to illustrate the versatility of the method. One is a 2-D pin-jointed truss with 31 bars and the other is a 3-D truss representative of an offshore platform. The latter is also used to introduce ways of improving the computational efficiency of the search. In all cases, frequency changes for the first ten modes are used in the calculations.

3.2. THIRTY-ONE-BAR TRUSS

The 31-bar truss, shown in Figure 1, was modelled using 31 classical consistent finite elements without internal nodes [17] giving 25 degrees of freedom. Damage in the structure was introduced as a reduction in the stiffness of individual bars,

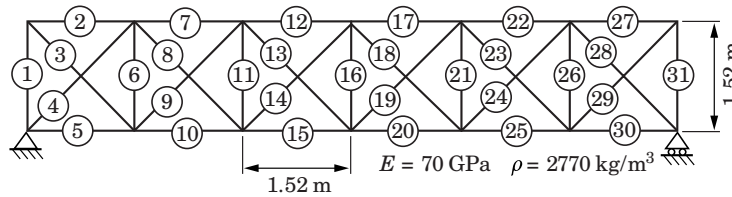


Figure 1. Thirty-one-bar truss structure.

TABLE 1
Damage scenarios for the 31-bar truss structure

Case 1		Case 2		Case 3	
Element	δD	Element	δD	Element	δD
11	25%	16	30%	1	30%
25	15%			2	20%

but the inertia properties were unchanged. This damage model agrees with others present in the literature [5, 11, 13] and is consistent with the MDLAC formulation.

Three different damage states were considered (see Table 1) and, for each of them, the true frequency changes $\{\Delta f\}$ were obtained by re-running an eigensolution. The predictions of the absolute damage levels using the first and second order approximations are shown in Figure 2.

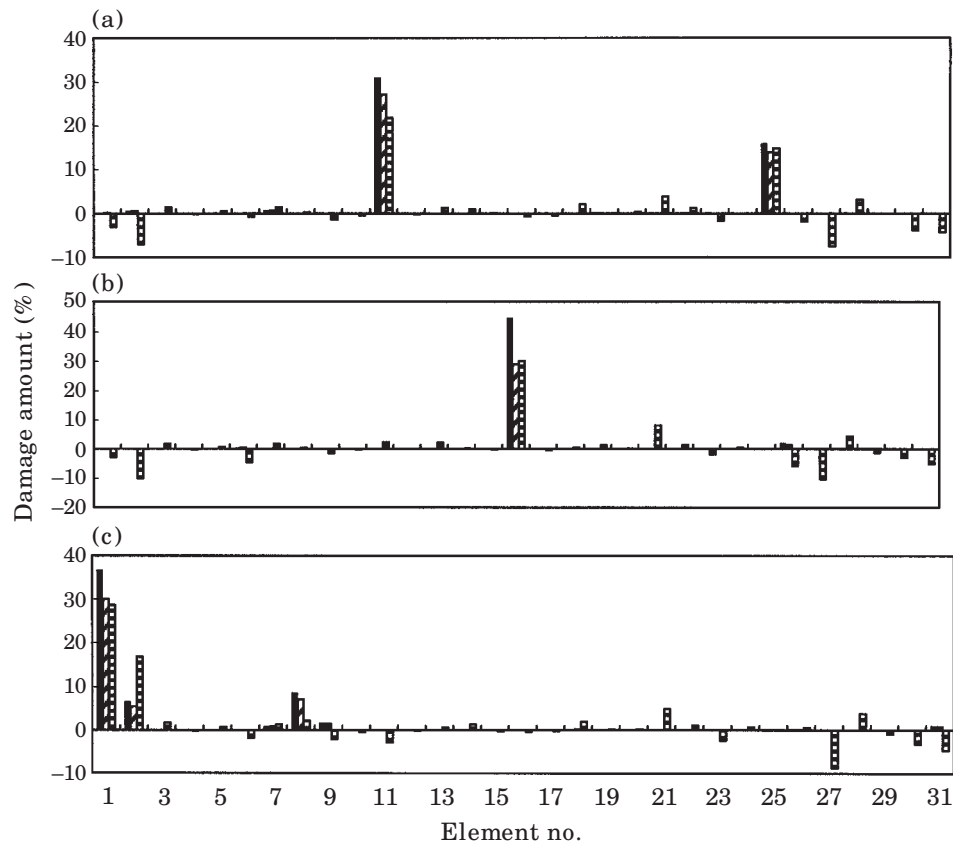


Figure 2. Damage location charts for the 31-bar truss structure. (a) Case 1: $\delta D_{11} = 25\%$, $\delta D_{25} = 15\%$, 10 modes; (b) Case 2: $\delta D_{16} = 30\%$, 10 modes; (c) Case 3: $\delta D_1 = 30\%$, $\delta D_2 = 20\%$, 10 modes. ■, 1st order MDLAC; ▨, 2nd order MDLAC; ▤, Pandey and Biswas.

The MDLAC results are also compared with the method presented by Pandey and Biswas [11]. They used complete mode shapes to estimate the flexibility matrices in the undamaged and damaged conditions using the expression:

$$[\mathbf{F}] = \sum_{k=1}^p \frac{1}{\omega_k^2} \{\boldsymbol{\phi}_k\} \{\boldsymbol{\phi}_k\}^T. \quad (10)$$

The change in the flexibility matrix was then written in the form:

$$[\Delta \mathbf{F}] = - \sum_{j=1}^m [\mathbf{F}]_{\text{Damaged}} [\mathbf{K}_j]^p [\mathbf{F}]_{\text{Undamaged}} \delta D_j. \quad (11)$$

Equation (11) resulted in a set of linear equations which can be solved for the absolute damage vector $\{\delta \mathbf{D}\}$.

For Case 1 (Figure 2(a)), all three approaches correctly identify the location of the two damage sites. The MDLAC prediction using the second order approximation gives more accurate predictions of the damage levels than either the first order approximation or the Pandey and Biswas method. A spread effect is also apparent with the latter, in that it incorrectly predicts small amounts of damage (some of which indicate an increase in stiffness) at other sites. Similar observations apply to Case 2 (Figure 2(b)) and to many other cases which have been investigated. In a few cases, however, the Pandey and Biswas method has been found to give better results as, for example, in Case 3 (Figure 2(c)) where the MDLAC approach underestimates the amount of damage in element 2 and gives a false indication of damage in element 8.

It can be concluded that the MDLAC approach using either first or second order approximations is able to assess the size of damage with good accuracy. It should be noted that for both sizing methods, the linear approximation of equation (3) is used for detecting the location(s) of damage. Equation (4) constitutes a statistically sound method for comparing two patterns and it is found that the MDLAC parameter is close to unity, even when the true frequency-damage relationship is non-linear, and thus provides a sound statistical measure of the contribution of different damaged locations to the overall frequency-change pattern.

While the second order sizing algorithm gives significantly better results for damage levels in excess of about 20%, the computational simplicity of the first order approximation makes it attractive for the level of precision typically required in practical damage monitoring applications.

The second order approximation is generally at least as good as the Pandey and Biswas method. This is significant since the latter requires complete mode shape information for both the damaged and undamaged states in order to calculate changes to the flexibility matrix. This is unattractive in practice since it implies either a comprehensive modal survey each time a damage evaluation is needed, or the use of a model expansion technique to obtain the required data. Either way, it is felt that the MDLAC approach offers a sound, cost-effective solution.

3.3. OFFSHORE PLATFORM STRUCTURE

The tubular steel offshore platform structure shown in Figure 3 was modelled with 76 two-noded 3-D Euler–Bernoulli beam elements giving a total of 372 degrees of freedom. The overall height of the platform is 83 m and the base is 45 by 42 m. Details of the geometry of the legs and cross-members are given in reference [18].

Even though the longest part of the overall diagnosis process is normally the collection of the required experimental data, it is recognized that the search for the maximum in $\{\delta\mathbf{D}\}$ -space can be a computationally intensive exercise if the number of potential damaged sites is large. One reason is that the linear assumption embodied in equation (3) implies an infinite number of maxima for the MDLAC function in the search range; all having the same relative proportion of damage in each element. It follows that, if the initial value for the maximum search is the undamaged state (i.e., near zero in $\{\delta\mathbf{D}\}$ -space), it is not necessary to search the whole of the domain of the stiffness reduction factor between 0 and 1. In this work all the assessments have been done in the range from 0 to 0.5.

While this restriction provides a useful time saving, the key factor determining the search time is the size of the $\{\delta\mathbf{D}\}$ vector; in other words, on the number of potential damaged locations included in the search. Significant time savings can be obtained if it is possible to limit the search to a sub-set of possible damage sites.

The MDLAC approach is based on the pattern recognition principle that damage at a particular location produces larger changes in some natural frequencies than in others. This, of course, is quantified in the sensitivity matrix $[\mathbf{S}]$. If it can be assumed that damage is present at only a few locations (i.e., that most of the structure remains undamaged), the large values found in the measured frequency-change vector $\{\Delta\mathbf{f}\}$ can be used in conjunction with the sensitivity

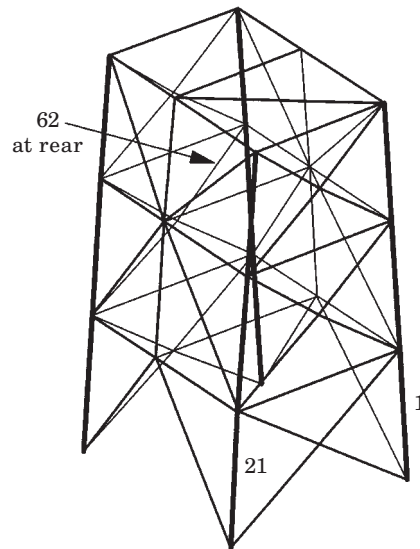


Figure 3. Offshore platform structure.

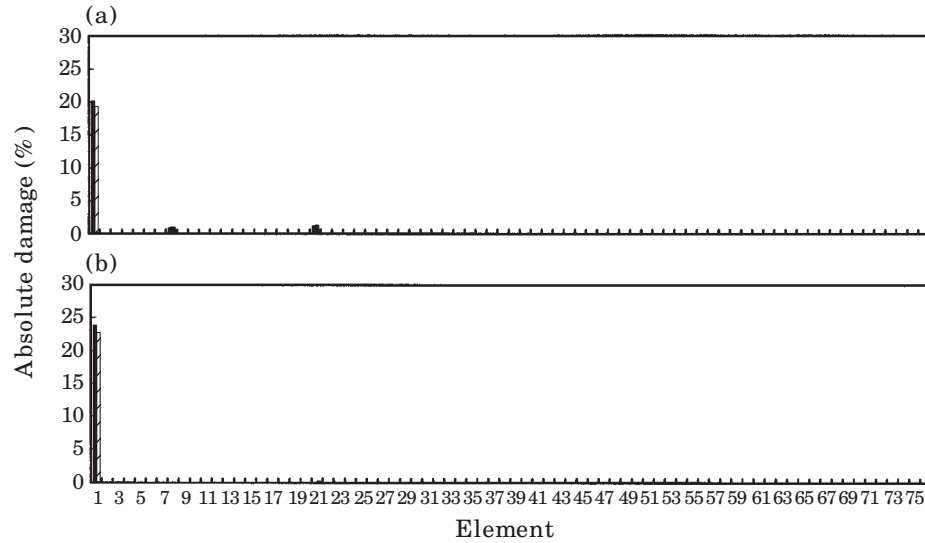


Figure 4. Damage location charts for the platform structure (Case 1); $\delta D_1 = 20\%$. (a) Full search of all 76 elements: 5776 iterations; (b) selective search of seven elements: 91 iterations. ■, 1st order; ▨, 2nd order.

matrix to identify locations which are more likely than others to produce such changes. For example, if it was found that mode 7 had the largest percentage frequency change, it might be expected that locations which would produce large changes in that frequency (as indicated by the sensitivity matrix) would be among the likely damage sites. In a multiple-damage situation, it is necessary to consider several of the modes whose frequencies change significantly and, for each, to identify a list of probable damage sites. Any restriction of the set of locations to be searched risks omitting one or more which are damaged and this is particularly true if many sites are damaged. However, if several modes are examined the resulting list of possible damage sites can be large enough to minimize this risk and, as will be illustrated later, even modest reductions in the number to be searched can produce significant savings.

To illustrate the benefits, the case of a 20% stiffness reduction to element 1 of the platform is considered. The results of a full search of all 76 elements using the frequency changes in the first ten modes is shown in Figure 4(a), where it can be

TABLE 2
Reduction in the number of iterations required

Number of modes	Number of locations per mode	Number of locations searched	Number of iterations
10	76	76	5776
5	10	32	1388
4	7	16	705
1	7	7	91

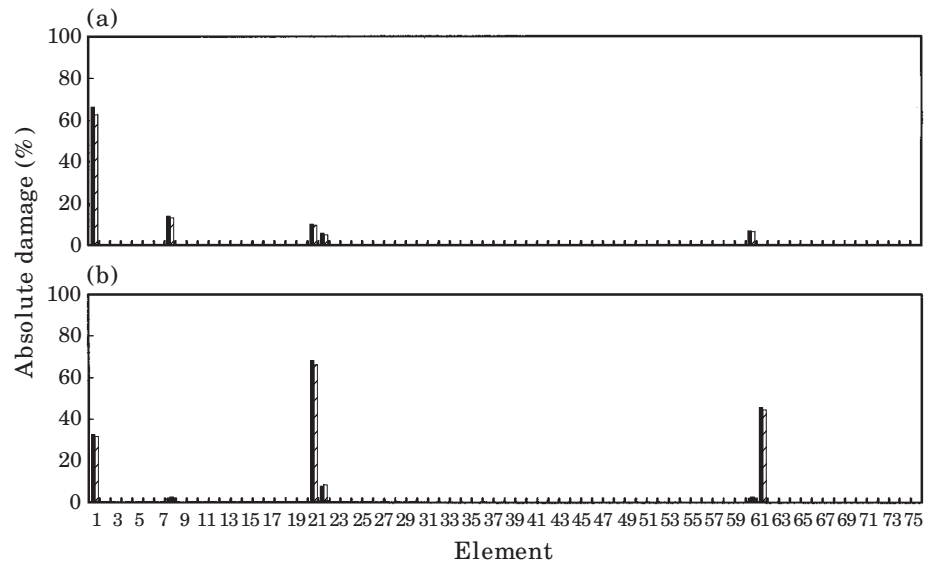


Figure 5. Damage location charts for the platform structure. (a) Case 2: $\delta D_1 = 60\%$; (b) Case 3: $\delta D_1 = \delta D_{21} = \delta D_{62} = 40\%$. ■, 1st order; ▨, 2nd order.

seen that both first and second order approximations give good predictions of the damage scenario. The search required 5776 iterations to converge.

Examining the five modes showing the largest frequency changes, and identifying ten locations with the highest damage sensitivities for each, gave a list (after eliminating duplicates) of 32 possible damage sites. Restricting the search to these locations took 1388 iterations and gave a location chart which was indistinguishable from Figure 4(a). These and two other cases are listed in Table 2. In the final row where the search list was reduced to just seven locations, only 91 iterations were required. Since the time needed for each iteration is also reduced, the overall time saving is over 500:1 compared with the full search. The result of the final search case is shown in Figure 4(b) where it will be seen that there is a small deterioration in the accuracy of the damage size prediction. The use of the MDLAC approach is illustrated by results for two further damage scenarios that are given in Figures 5(a) and (b). For Case 2 (Figure 5(a)), a 60% stiffness reduction was imposed on element 1 and for Case 3 (Figure 5(b)), a 40% stiffness reduction was imposed on elements 1, 21 and 62. In each case, the correct damage locations are found, with good indications of the size of the stiffness reduction.

4. DISCUSSION OF THE ANALYTICAL CASES

In each of the cases presented, it is found that the MDLAC approach gives good predictions of the location of both single and multiple damage sites and of the absolute stiffness reduction. To the authors' knowledge, it is the only method based on monitoring only the changes in the natural frequencies which is able to predict both the location and absolute extent of damage. As mentioned in the introduction, this feature makes it particularly attractive for practical applications.

For damage in excess of about 20%, it has been found that MDLAC can give inaccurate size predictions due to the non-linear relationship between frequency changes and damage. In particular, the solution frequency-change vector, $\{\delta \mathbf{f}(\{\delta \mathbf{D}\})\}$, is not an exact match to the “measured” vector, $\{\Delta \mathbf{f}\}$. Despite this, the method still predicts the true damage locations.

The method of pre-selecting probable damage locations discussed in section 3.3 provides significant time savings during the search for the maximum MDLAC value, but has to be used conservatively to avoid omitting any of the true damage locations from the search list.

5. EXPERIMENTAL VALIDATION

5.1. TEST STRUCTURE

It is clear that large errors in the measured frequencies could alter the apparent frequency-change pattern and affect the ability of the MDLAC approach to give a correct prediction. The other problem faced in practice is that the analytical FE model used to calculate the sensitivity and Hessian matrices is unlikely to be an exact match to the real structure. In principle, FE model updating could be applied to address the situation, but since the approach is intended for routine monitoring with minimum effort, it may be difficult to justify the additional cost. It was therefore felt that the use of a non-updated model would provide a more realistic (and more demanding) test of the method.

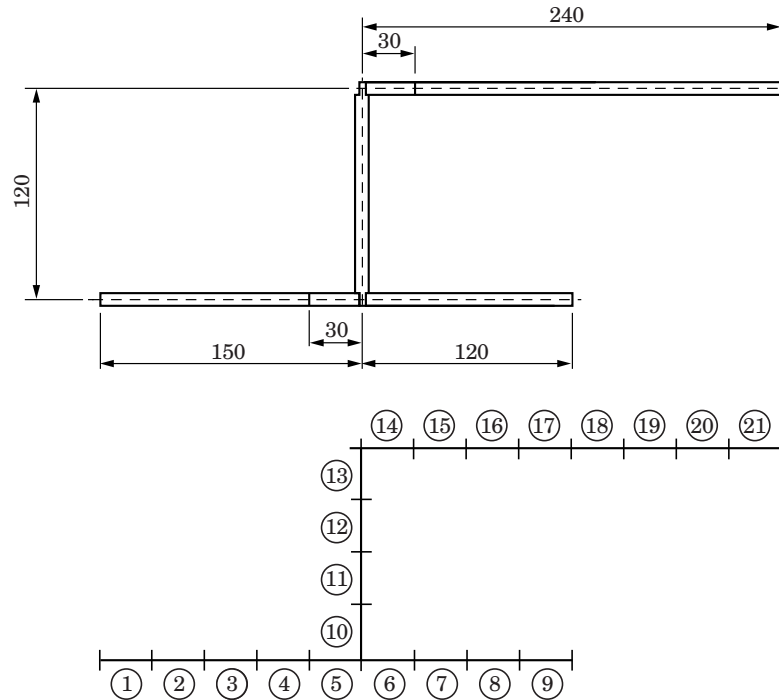


Figure 6. Aluminium rod test structure and its FE model. All dimensions in mm; all rods have a diameter of 7.9 mm.

The test structure used is shown in Figure 6 and consisted of a number of circular aluminium rods which could be screwed together to make a range of different configurations. Damage was simulated by substituting one or more of the sections by rods of the same length, but of smaller diameter. The FE model used to obtain the required sensitivity and Hessian matrices is also shown in Figure 6 and used 21 two-noded 3-D beam elements giving 132 degrees of freedom.

For the undamaged structure, single-input multiple-output impact tests (using two accelerometers to sense the in-plane and out-of-plane motions) were used to measure frequency response functions (FRFs) at the 22 points corresponding to the nodes on the FE model. These were processed using a poly-reference curve-fitter to give the first 12 natural frequencies and mode shapes. For the damaged cases, measurements were taken at just five points, from which it was possible to match the mode shapes with the undamaged state.

5.2. EXPERIMENTAL RESULTS

Table 3 lists the measured natural frequencies of the first 12 modes of the undamaged structure together with the values predicted by the FE model. It will be seen that significant differences exist in a number of the frequencies.

Four damage scenarios were investigated. For Cases 1, 2 and 3, the 30-mm long section of rod corresponding to element 5 was reduced to diameters of 7.00, 6.00 and 5.00 mm, respectively. For Case 4, elements 5 and 14 were both reduced to a diameter of 7.00 mm. Since the measured mode shapes are dominated by bending and torsional motion, the effective stiffness reduction is given by the second moments of area. It follows that the above diameter reductions are equivalent to stiffness reductions of 40, 67 and 84%, respectively.

Table 4 gives the measured percentage reduction in each natural frequency for the four cases. It can be seen that a few of the smaller values in Table 4 are

TABLE 3
Experimental and numerical frequencies of the undamaged structure ($E = 52$ GPa, $G = 21$ GPa, density = 2900 kg/m³)

Mode no.	Experimental (Hz)	Numerical (Hz)	Difference (%)
1	86.4	88.0	+1.8
2	95.9	93.8	-2.1
3	196.0	214.7	+9.6
4	312.7	323.4	+3.4
5	379.6	374.2	-1.4
6	468.8	482.1	+2.8
7	489.5	499.3	+2.0
8	1144.0	1046.6	-8.5
9	1149.5	1100.9	-4.2
10	1211.0	1150.1	-5.0
11	1278.8	1245.9	-2.6
12	1574.2	1475.4	-6.3

TABLE 4

Experimental percentage frequency reductions for the four damage cases

Mode no.	Case 1 ($\delta D_5 = 40\%$)	Case 2 ($\delta D_5 = 67\%$)	Case 3 ($\delta D_5 = 84\%$)	Case 4 ($\delta D_5 = \delta D_{14} = 40\%$)
1	0.4	1.9	12.7	5.5
2	1.5	5.6	18.3	5.3
3	5.5	16.5	35.8	7.9
4	2.7	7.8	50.1	2.6
5	5.2	17.8	19.3	4.9
6	-0.5	-0.5	2.6	-0.9
7	-0.1	0.1	4.7	2.0
8	0.9	4.6	15.6	0.6
9	0.5	3.3	14.1	0.7
10	0.1	0.8	2.4	0.2
11	0.4	0.7	2.3	0.8
12	0.1	0.8	5.2	-1.3

negative, indicating a frequency increase. While this may in part be associated with experimental error, examination of the mode shapes confirmed that these modes would not be sensitive to stiffness changes in the elements chosen. As a result, the mass loss due to the diameter reduction has a greater effect than the loss of stiffness; a conclusion also confirmed by tests with the FE model. The mass loss effect will be present in all cases, of course, but is ignored by the MDLAC formulation that is based on reductions in stiffness only. The fact that the approach is able to diagnose the damage situation effectively is a further measure of its robustness.

Figure 7 shows the location charts for three of the experimental cases. For Case 1, with a 40% stiffness reduction in element 5, the MDLAC algorithm correctly identified element 5 as having the highest damage level (Figure 7(a)), but also indicated some damage in elements 10 and 11. It will be seen from Figure 6 that these are adjacent to element 5. The spatial discrimination of the prediction of the damaged site depends to a large extent on the wavelength of the modes affected. It will be seen from Table 4 that modes 3, 4 and 5 have the largest frequency changes and these have long wavelengths compared with the lengths of the elements used in the FE model. In principle, the resolution could be improved by involving more modes in the analysis, but the prediction does not improve with all 12 modes and, since the method is intended as a simple diagnostic tool, 12 modes was felt to be a realistic practical limit. The result does, however, give a sufficiently clear indication of the area of the damage to allow visual inspection to confirm the precise location of the problem. This level of spatial discrimination would be more than adequate in many practical applications.

The predicted size of the damage is less than the true level, with the second order approximation being less accurate than the first order. Since the experiment imposed mass loss in addition to stiffness reduction, the measured frequency reductions were less than those for a stiffness reduction alone. This smaller

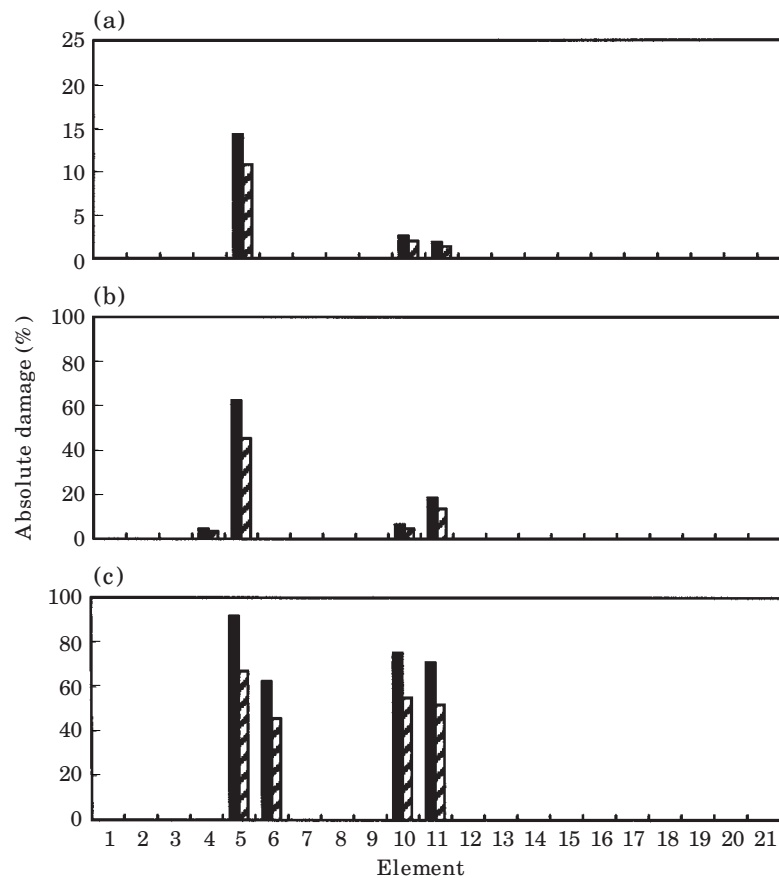


Figure 7. Damage location charts for experimental Cases 1, 2 and 3. (a) Case 1: $\delta D_5 = 40\%$, 10 modes; (b) Case 2: $\delta D = 67\%$, 10 modes; (c) Case 3: $\delta D = 84\%$, 10 modes. ■, 1st order; ▨, 2nd order.

frequency reduction is reflected in the lower damage level indicated by the sizing algorithm.

Case 2, with a 67% stiffness reduction in element 5, gives a similar result (Figure 7(b)), with the highest damage level again predicted in element 5 and lower levels in the adjacent elements 4, 10 and 11. The predicted extent is closer to the true value in this case, confirming that the reduction in stiffness has a more significant effect on the frequency changes than the loss of mass.

Case 3, with an 84% stiffness reduction in element 5, again correctly predicts the damaged area (Figure 7(c)). While element 5 is still predicted to have the largest damage, significant levels are also predicted in the adjacent elements 6, 10 and 11. This spread effect is a consequence of the linear assumption in the MDLAC formulation, coupled with the large 84% stiffness reduction present.

For Case 4, 40% stiffness reductions were imposed at both elements 5 and 14 and it will be seen from Figure 8(a) that both areas are correctly predicted (elements 5 and 10 and elements 13 and 14). The predictions used data from the first ten modes. As with Case 1, which also had a 40% reduction, the predicted

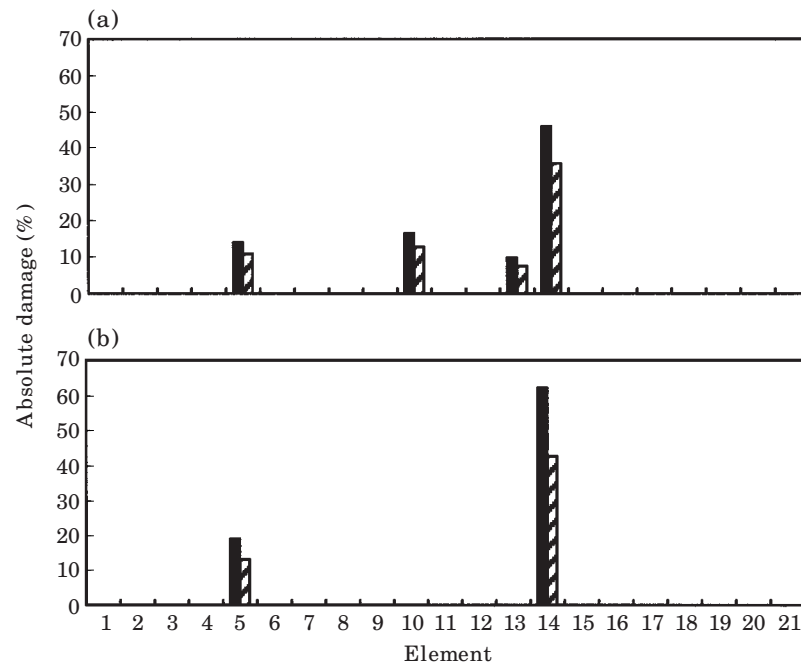


Figure 8. Damage location charts for experimental Case 4, $\delta D_5 = \delta D_{14} = 40\%$. (a) 10 Modes; (b) 12 modes. ■, 1st order; ▨, 2nd order.

level is underestimated due again to the fact that the sensitivity matrix in the MDLAC algorithm assumes no mass loss. Unlike Cases 1 to 3, the prediction for Case 4 is improved if all 12 modes are made available, as can be seen from Figure 8(b).

The tests provide good validation of the method. While it is difficult to quantify the errors in the individual frequencies, they are obtained from global estimates from several FRFs. It is important to note that a non-updated model was used to compute the sensitivity matrix and it is clear from the differences in the frequencies in Table 3 that significant modelling errors exist. Despite this, the predictions are good. This is because, while the measured and model frequencies may be different, the pattern of the frequency changes is similar.

6. CONCLUSIONS

A new correlation coefficient termed the Multiple Damage Location Assurance Criterion (MDLAC) has been shown to provide reliable information about the location and absolute size of damage at one or more sites. It has the practical attraction of only requiring information about the changes in a few of the natural frequencies between the undamaged and damaged states. A further advantage is that the initial modal survey to find the undamaged structure's frequencies and mode shapes need only be carried out in sufficient detail to provide a match with the FE model. Since only about ten modes are needed, the number of FRF measurements required is modest. Subsequent checks for damage would require

even fewer measurements in order to establish the changes in the natural frequencies.

First and second order methods have been developed to estimate the absolute damage extent. While the second order approach generally gives better results, it is felt that the first order method is likely to be adequate for routine condition monitoring purposes where precise knowledge of the defect size is less important than its location.

The matrix used in the formulation for describing the sensitivity of each natural frequency to small reductions in local stiffness from the undamaged state can be obtained efficiently using equation (3) and requires only one eigen-solution of the FE model of the structure. The same is true of the Hessian matrices used for the second order estimate of the absolute amount of damage.

The experimental evidence suggests that an updated model is not necessary in order to obtain satisfactory predictions in practice.

REFERENCES

1. A. MESSINA, I. A. JONES and E. J. WILLIAMS 1996 *Proceedings of Conference on Identification in Engineering Systems, Swansea, U.K.*, 67–76. Damage detection and localisation using natural frequency changes.
2. C. R. FARRAR and K. M. CONE 1995 *Proceedings of the 13th International Modal Analysis Conference* **1**, 203–209. Vibration testing of the I-40 bridge before and after the introduction of damage.
3. A. BERMAN and E. J. NAGY 1983 *American Institute of Aeronautics and Astronautics Journal* **21**, 1168–1173. Improvement of a large analytical model using test data.
4. G. LALLEMENT, A. RAMANITRANJA and M. COGAN 1996 *Proceedings of Conference on Identification in Engineering Systems, Swansea, U.K.*, 338–356. Optimal sensors deployment: applications to model updating problems.
5. P. CAWLEY and R. D. ADAMS 1979 *Journal of Strain Analysis* **14**, 49–57. The location of defects in structures from measurements of natural frequencies.
6. J. E. T. PENNY, D. WILSON and M. I. FRISWELL 1993 *Proceedings of the 11th International Modal Analysis Conference* **1**, 861–867. Damage location in structures using vibration data.
7. E. J. WILLIAMS, T. CONTURSI and A. MESSINA 1996 *Proceedings of Conference on Identification in Engineering Systems, Swansea, U.K.*, 368–376. Damage detection and localisation using natural frequency sensitivity.
8. M. BISWAS, A. K. PANDEY and M. M. SAMMAN 1990 *The International Journal of Analytical and Experimental Modal Analysis* **5**, 33–42. Diagnostic experimental spectral/modal analysis of a highway bridge.
9. O. LOLAND and C. J. DODDS 1976 *Proceedings of the 8th Annual Offshore Technology Conference* **2**, 313–319. Experiences in developing and operating integrity monitoring system in North Sea.
10. J. K. VANDIVER 1975 *Proceedings of the 7th Annual Offshore Technology Conference* **2**, 243–252. Detection of structural failure on fixed platforms by measurements of dynamic response.
11. A. K. PANDEY and M. BISWAS 1995 *The International Journal of Analytical and Experimental Modal Analysis* **10**, 104–117. Damage diagnosis of truss structures by estimation of flexibility change.
12. D. C. ZIMMERMAN and M. KAOUK 1994 *Journal of Vibration and Acoustics* **116**, 222–231. Structural damage detection using a minimum rank update theory.

13. K. G. TOPOLE and N. STUBBS 1995 *The International Journal of Analytical and Experimental Modal Analysis* **10**, 95–103. Non-destructive damage evaluation in complex structures from a minimum of modal parameters.
14. T. CONTURSI, A. MESSINA and E. J. WILLIAMS 1997 *Journal of Vibration and Control*, in press. A multiple damage location assurance criterion based on natural frequency changes.
15. A. MESSINA, T. CONTURSI and E. J. WILLIAMS 1997 *Proceedings of the 15th International Modal Analysis Conference* **1**, 658–664. Multiple damage evaluation using natural frequency changes.
16. R. M. LIN and M. K. LIM 1993 *Proceedings of the 11th International Modal Analysis Conference* **2**, 1554–1558. Methods for calculating derivatives of eigenvalues and eigenvectors.
17. M. PETYT 1990 *Introduction to Finite Element Vibration Analysis*. Cambridge, England: Cambridge University Press.
18. P. BROUGHTON and L. SILVA 1996 *Proceedings of the Institution of Civil Engineers, Structures and Buildings* **116**, 1–18. Design of the Judy steel piled jacket structure.